


Article

Investigation of the Temperature-Related Wear Performance of Hard Nanostructured Coatings Deposited on a S600 High Speed Steel

Eleonora Santecchia ^{1,2,*} , Marcello Cabibbo ³, Abdel Magid Salem Hamouda ⁴, Farayi Musharavati ⁴, Anton Popelka ⁵ and Stefano Spigarelli ³

¹ Consorzio Interuniversitario Nazionale per la Scienza e Tecnologia dei Materiali (INSTM—UdR Ancona), Via Brece Bianche 12, 60131 Ancona, Italy

² Dipartimento SIMAU, Università Politecnica delle Marche, Via Brece Bianche 12, 60131 Ancona, Italy

³ Dipartimento di Ingegneria Industriale e Scienze Matematiche (DIISM), Università Politecnica delle Marche, 60131 Ancona, Italy; m.cabibbo@univpm.it (M.C.); s.spigarelli@univpm.it (S.S.)

⁴ Mechanical and Industrial Engineering Department, College of Engineering, Qatar University, PO Box 2713 Doha, Qatar; hamouda@qu.edu.qa (A.M.S.H.); farayi@qu.edu.qa (F.M.)

⁵ Center for Advanced Materials, Qatar University, PO Box 2713 Doha, Qatar; anton.popelka@qu.edu.qa

* Correspondence: e.santecchia@univpm.it; Tel.: +39-0712204751

Received: 31 January 2019; Accepted: 9 March 2019; Published: 15 March 2019



Abstract: Thin hard coatings are widely known as key elements in many industrial fields, from equipment for metal machining to dental implants and orthopedic prosthesis. When it comes to machining and cutting tools, thin hard coatings are crucial for decreasing the coefficient of friction (COF) and for protecting tools against oxidation. The aim of this work was to evaluate the tribological performance of two commercially available thin hard coatings deposited by physical vapor deposition (PVD) on a high speed tool steel (S600) under extreme working conditions. For this purpose, pin-on-disc wear tests were carried out either at room temperature (293 K) or at high temperature (873 K) against alumina (Al₂O₃) balls. Two thin hard nitrogen-rich coatings were considered: a multilayer AlTiCrN and a superlattice (nanolayered) CrN/NbN. The surface and microstructure characterization were performed by optical profilometry, field-emission gun scanning electron microscopy (FEGSEM), and energy dispersive spectroscopy (EDS).

Keywords: high speed steel; nanostructured coatings; thin films; FEGSEM; tribology

1. Introduction

The evolution of industrial processes makes them faster and more demanding from a material resistance point of view. This draws attention to the technological and environmental issues that still affect the crucial production steps such as cutting and machining. From an environmental point of view, limiting or avoiding the use of lubricating oils for machining and forging operations is a key issue [1–3]. Concerning the perspectives of productivity and cost-effectiveness, there are different critical factors that certainly deserve to be considered, such as: (i) the need to increase the productivity by raising the cutting speed, (ii) the need to extend the lifetime of tools, and (iii) the need to lower the cost of tooling, which is typically in the range of 2–5% of the total manufacturing costs [4].

A feasible way to reach these goals is the implementation of thin hard coatings with specific mechanical properties, such as good wear, scratch and corrosion resistance, as well as attractive colors [5,6]. Thin hard coatings have been successfully employed in a variety of applications, from tools, dies, and molds to aerospace and automotive fields [4,7–10]. Moreover, the deposition of hard and tough coatings helps prevent brittle failure when tools are subjected to external stresses [11] and,

as extensively documented in the literature [12–18], the nanostructure of thin hard coatings has a remarkable influence on their tribological behavior.

Common techniques available to modify the cutting tool substrate include chemical vapor deposition (CVD) and physical vapor deposition (PVD) [19]. Nowadays, PVD technology is preferred over CVD due to the lower operating temperature and the inner environmentally friendly nature of the process [20,21].

Nitride-based hard coatings, obtained by a number of PVD processes, have found increasing applications owing to their combination of remarkable properties such as: (i) a high degree of hardness, (ii) excellent wear resistance, and (iii) corrosion resistance [22,23]. TiN was the first commercial PVD coating, firstly deposited back in the early 1980s [24]. This coating system was followed by TiN/Ti(CN), known as the first multilayer PVD coating [25,26]. The technological evolution of these coatings continued with the stoichiometric TiAlN [27] and other binary and ternary compounds made up of Ti, Al, and Cr [4,28–35]. All these coatings showed excellent oxidation resistance [36,37] and good mechanical properties [38]. In particular, superior surface properties have been reported in the literature for the AlTiCrN coating [39] due to the formation of a protective layer made up of stable and dense $\alpha(\text{Al,Cr})_2\text{O}_3$ mixed oxides, which make it suitable for applications involving temperatures as high as 1100 °C [21].

A further development of the mechanical and tribological properties of hard coatings as well as to their range of applicability has been achieved by adding other elements and tailoring the properties of the thin films at an atomic level by designing and producing nanocomposite coatings (Ti–Si–N, Al–Ti–Si–N, and Ti–B–N) [4,40,41]. Starting from the intuition of Koehler [42] and owing to the subsequent pioneering work of Helmersson et al. [43], remarkable improvements were possible in the development of superlattice structured hard coatings, which are obtained by the deposition of alternate nanolayers of two materials having the same crystal structure. The high degree of hardness achieved (exceeding even 50 GPa [43,44]) is given by the interfaces between layers, acting as energy barriers that counteract the motion of dislocations [45,46]. Several nanolayered superlattice hard coatings have already been tested in recent years, including TiN/NbN, TiAlN/CrAlN, and CrN/NbN, as an environmentally friendly replacement for hard chromium [47–60]; moreover, these have shown good wear resistance [61].

The evolution of conventional hard coatings for cutting tool applications has been intensively investigated [62] and the market's requests to increase productivity and sustainability (i.e., through the reduction of lubricants) of the machining processes, together with reduced costs and lead time [63], suggest the need to fully exploit the potential of advanced hard coatings, which are already available, in order to evaluate their potential use for cutting tool applications. Therefore, the aim of the present paper is to investigate the dry sliding wear performance of two commercially available coatings—a multilayer AlTiCrN and a superlattice (nanolayered) CrN/NbN deposited on a S600 high speed steel. The peculiar architectures of the chosen coatings make them suitable for technologically challenging applications and since coatings for cutting tools typically need to withstand mechanical and thermal loads, tribology tests (tribotests) were performed at room temperature (RT, 293 K) and high temperature (HT, 873 K). Given the results reported on the thermal stability of these two coatings published by some of the authors in the present study [64], where the superlattice coating showed degradation of its mechanical properties at around 873 K, this temperature was chosen as the highest to be set in order to evaluate the tribological performance of the two commercially available coatings. The results of the dry sliding tests were discussed and analyzed using coupling optical profilometry, field emission gun scanning electron microscopy (FEGSEM), and energy dispersive spectroscopy (EDS) techniques.

2. Materials and Methods

Flat discs (30 mm in diameter) of S600 high speed steel (HSS), hardened to 61–63 HRC and lapped to $R_a < 0.04$ mm, were used as substrates. The coatings were deposited by the cathodic-arc evaporation PVD method and their chemical and structural characteristics are reported in Table 1 [64]. Samples

were taken from the standard industrial production line of the Lafer[®] company (Piacenza, Italy), and further details can be found in Reference [65].

Table 1. Composition and characteristics of the coatings (as-deposited conditions).

Coating	Chemical Composition	Structure	Deposition Temperature (K)	Thickness (μm)	Hardness (HV 0.025)	Max Operating Temperature (K)
AlTiCrN	$\text{AlTiCr}_x\text{N}_{1-x}$	multilayer	693	2.92	3300	1123
CrN/NbN	$\text{Cr}_{0.336}\text{Nb}_{0.182}\text{N}_{0.482}$	nanolayer	553	2.61	3000	1373

The multilayer structure of the AlTiCrN coating was obtained through a layer-upon-layer deposition in planar mode so that the bond between atoms belonging to different layers was not exactly the same as that existing between atoms of the same horizontal layer. This peculiar arrangement differentiates this coating from typical monolayers of AlTiCrN. The chemical composition of this coating was measured with an X-ray microanalysis device within a scanning electron microscope and was found to be the following: $\text{AlTiCr}_{0.3}\text{N}_{0.7}$. The superlattice coating was obtained through the deposition of alternating layers of CrN and NbN with a period of 4 nm. It is worth noting that while the AlTiN system with chromium added is well known for high temperature applications [66–69], the CrN/NbN system has been recently proposed for this purpose [70–72].

Tribotests were performed using a high temperature pin-on-disc tribometer (VTHT, Anton-Paar[®], Graz, Austria). The coatings were subjected to wear tests at room temperature (RT, 293 K) and high temperature (HT, 873 K).

All the tests were performed in air using alumina balls (Al_2O_3) with a diameter of 6 mm as counterparts, under a normal load of 12 N. The coated discs were rotated at a fixed speed of 538 rpm (~ 45.07 cm/s), with a track radius of 8 mm, and covered a total sliding distance of 5000 m (which led to a duration of about 3 hours for each test). The rotational speed of the wear measurement was chosen according to the literature [73–76] to generate a challenging set of testing conditions, which can approximate a technologically demanding work environment for tools for the dry machining condition. Moreover, owing to the other parameters of the tribometer, this linear speed value was the highest achievable by the system. For the HT wear tests, each sample was mounted and fixed to the holder and, by turning on the heating system (tubular furnace inside the equipment), the sample was exposed to HT for a constant time interval before the test started to ensure that its entire volume was at the same temperature level at the beginning of the sliding contact. A minimum of three tribotests were conducted for each condition.

In order to characterize the samples, high-resolution FEGSEM observations and EDS inspections were carried out on a Zeiss[®] Supra 40 FEGSEM (Carl Zeiss Microscopy GmbH, Jena, Germany) equipped with a Bruker[®] Quantax 200 microanalysis (Bruker Nano GmbH, Berlin, Germany). FEGSEM observations were performed by collecting the secondary electrons (SE) signal with the in-lens detector, while elemental line scanning and spectra were used for the EDS analyses. The profiles of the wear tracks were acquired with an optical surface metrology system Leica DCM8 (Leica Microsystems, Wetzlar, Germany) in three different positions. Finally, the specific wear rate W was calculated using the normal load N , the sliding distance S , and the wear volume V [66,77], which was calculated using the wear track depth and width information from the profiles examined at the optical profilometer.

3. Results

The surface of the as-deposited samples was investigated by FEGSEM and the results are shown in Figure 1.

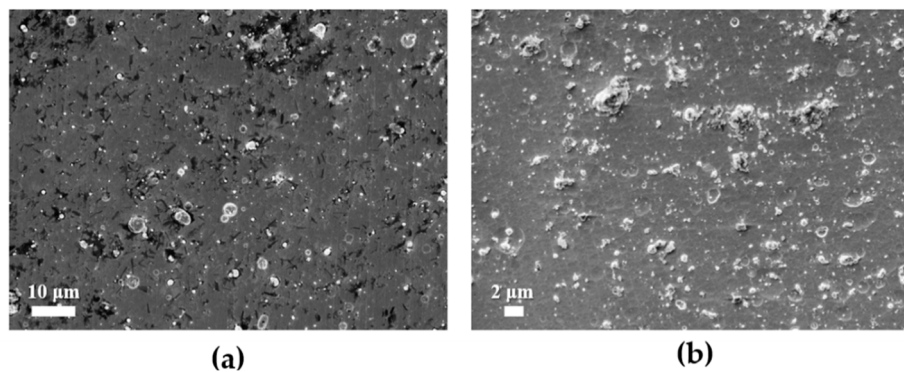


Figure 1. Field emission gun scanning electron microscopy (FEGSEM) inspection of the samples surface: (a) AlTiCrN, (b) CrN/NbN.

The micrographs in Figure 1 revealed a high concentration of droplets on the surface of both samples, although this effect was more pronounced in the case of the AlTiCrN coating (Figure 1a), both in terms of droplet size and frequency (the micrographs in Figure 1 were taken using different magnifications). The presence of these droplets can be ascribed to the insufficient reaction between metal macroparticles and nitrogen during the cathodic arc-evaporation process [67].

The results of the tribotests are shown in Figure 2, where the evolution of the coefficient of friction (COF) with the linear sliding distance, representative of the behavior of all the samples, is reported.

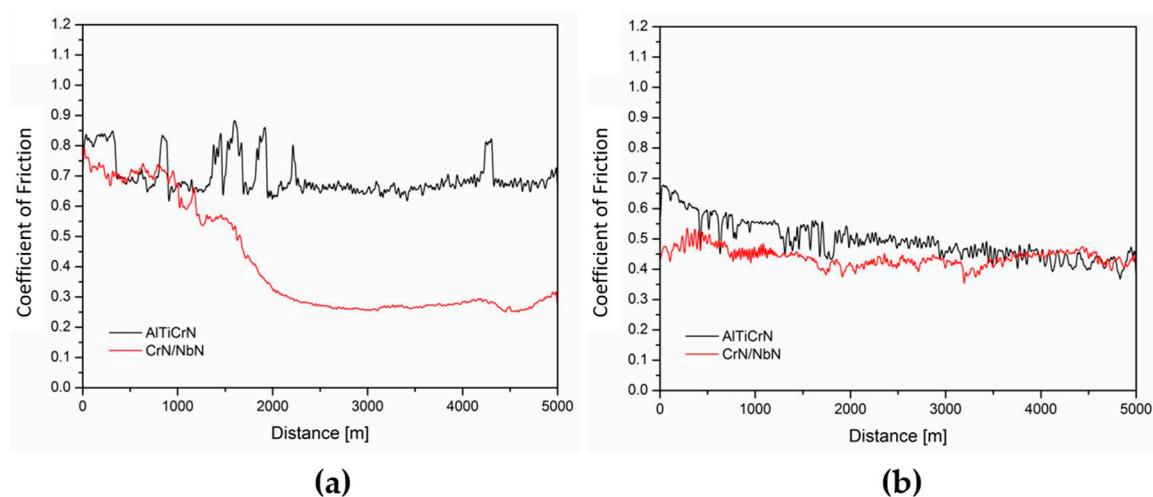


Figure 2. Coefficient of friction at: (a) room temperature and (b) high temperature. Black lines correspond to AlTiCrN and red ones to CrN/NbN.

The black lines in Figure 2 describe the behavior of the AlTiCrN coatings, while the red lines describe that of the CrN/NbN coatings. At RT (Figure 2a), the multilayer coating showed a relatively stable COF value despite the presence of a few sparks. On the other hand, the superlattice coating showed a peculiar behavior during the RT tests under dry conditions characterized by a slight decrease between ~895 m and ~1635 m, followed by a steep and continuous COF reduction to ~0.26. A remarkable effect that is linked to the temperature level is the lower starting COF value at the very beginning of the HT wear tests (Figure 2b). This phenomenon is particularly relevant for the CrN/NbN coating with the difference in the COF starting value being about 0.35 compared to the RT test. Since a minimum of three tests were performed for each condition, the mean values of the COF calculated in the steady state regime were 0.66 ± 0.01 and 0.48 ± 0.02 for the AlTiCrN coating at RT and HT, respectively. For the RT tests of the CrN/NbN coating, the steady state regime can be identified as

the first part of the graph before the steep decrease due to the debris generation, and its value was 0.72 ± 0.01 , while for the HT test the mean value was 0.45 ± 0.03 .

In order to correlate the tribological results with the morphological and structural modifications of the coatings, FEGSEM inspections were performed on all samples after the tribotests, and the profiles of the wear tracks were acquired using the optical profilometry technique.

After the RT tribotests, the AlTiCrN coating showed a wear track characterized by parallel grooves oriented toward the sliding direction (Figure 3a). A relatively smooth profile is shown in Figure 3b, except for the debris accumulation on the inner side of the wear track. The severe temperature effect on the wear of this multilayer coating is clearly visible in Figure 3c, where high roughness and remarkable plastic deformation were detected, and in Figure 3d where the wear track profile showed that the coating had been removed in the contact area. Furthermore, a slight accumulation of wear debris (spallation) at both edges of the wear track was detected (Figure 3d), together with a larger dimension of the track.

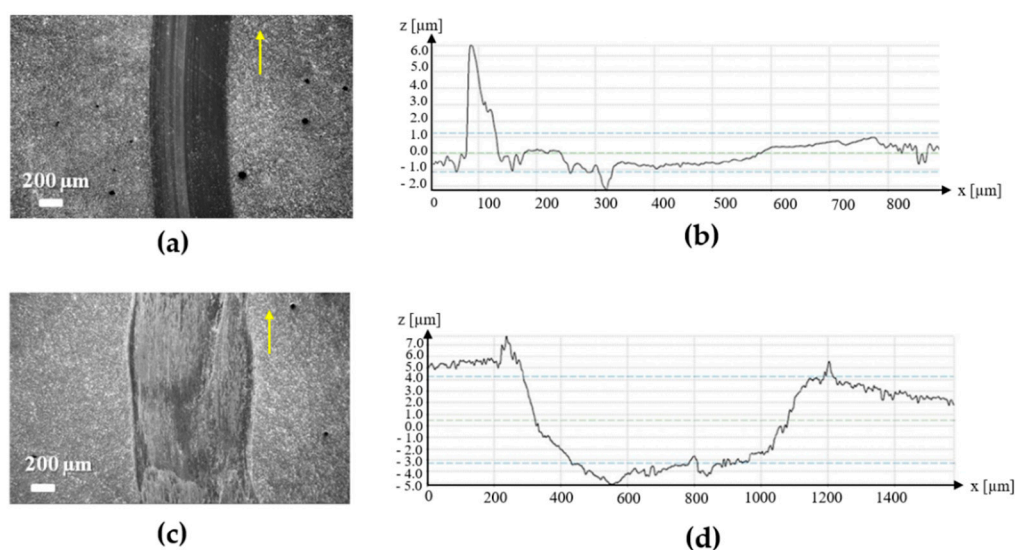


Figure 3. FEGSEM micrographs and wear track profiles of the AlTiCrN coatings after room temperature tribotests (a,b) and high temperature tribotests (c,d). Yellow arrows indicate the sliding direction during the wear test. In the diagrams on the right, z (μm) is the wear depth, while x is the wear track width (μm).

After the RT tribotest, a strong presence of deep grooves and wear debris were observed on the wear track of the CrN/NbN sample (Figure 4a). As can be seen from Figure 4c, the HT tribotest resulted in a remarkable plastic deformation of the coating in the position corresponding to the wear track, the dimension of which was also increased compared to the RT test (Figure 4a). The wear track profile taken after the RT tests (Figure 4b) showed coating removal at some points, corresponding to the deepest scratches in the wear track, while the profile acquired after HT tribotests (Figure 4d) highlighted the complete removal of the coating. EDS line scans were performed on the wear tracks of all the tested samples, and the most representative results are reported in Figure 5.

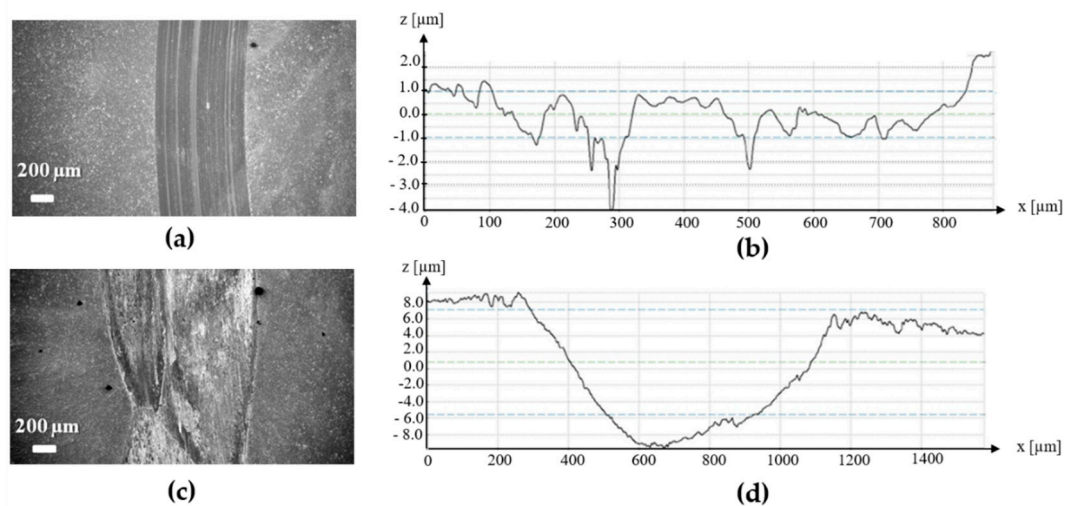


Figure 4. FEGSEM micrographs and wear track profiles of the CrN/NbN coatings after room temperature tribotests (a,b) and high temperature tribotests (c,d). In the diagrams on the right, z (μm) is the wear depth, while x is the wear track width (μm).

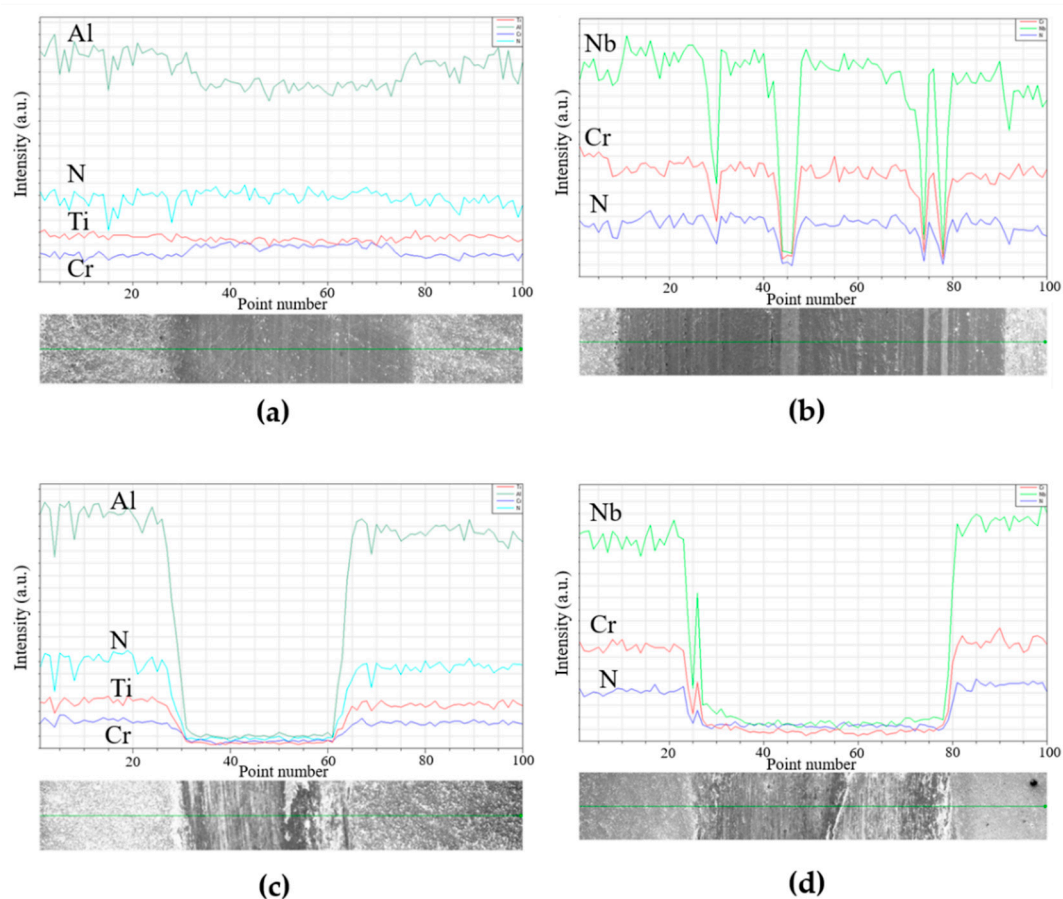


Figure 5. Energy dispersive spectroscopy (EDS) line scan of the samples after room temperature (RT, upper row) and high temperature (HT, lower row) tribotests: (a) AlTiCrN—RT, (b) CrN/NbN—RT, (c) AlTiCrN—HT, and (d) CrN/NbN—HT. The X-ray characteristics were generated by a 10 keV electron beam.

Figure 5a shows that the effect of the RT wear test on the AlTiCrN coating was negligible, with the concentrations of the elements being almost steady during the linear spatial scan. On the other

hand, the HT tribotest performed on AlTiCrN showed a complete removal of the coating (Figure 5c). A slight accumulation of wear debris at the edges of the wear track was also observed. After the RT test, the superlattice CrN/NbN coating showed that the removal of the coating had occurred at the deepest grooves of the wear track, a result which was confirmed by the steep drop-offs of the EDS line scans of the coating elements (Figure 5b). After the wear test at 873 K (Figure 5d), the coating experienced a dramatic wear with it being completely removed from the substrate by the end of the test. This effect was clearly shown by the EDS line scans of the elements, which also highlighted a spallation phenomenon of the coating that was particularly marked on one side of the wear track.

The profilometry results obtained for all the tested samples of each condition were used to calculate the wear volume according to the following equation (Equation (1)):

$$V = \frac{t}{2b} (3t^2 + 4b^2) 2\pi r \quad (1)$$

where r is the wear track radius, while t and b are the wear track depth and width, respectively.

The specific wear rate W (mm^3/Nm) was calculated using the normal load N , the sliding distance S , and the wear volume V [66] (Equation (2)):

$$W = \frac{V}{N \cdot S} \quad (2)$$

The results of the wear rate calculations are reported in Figure 6.

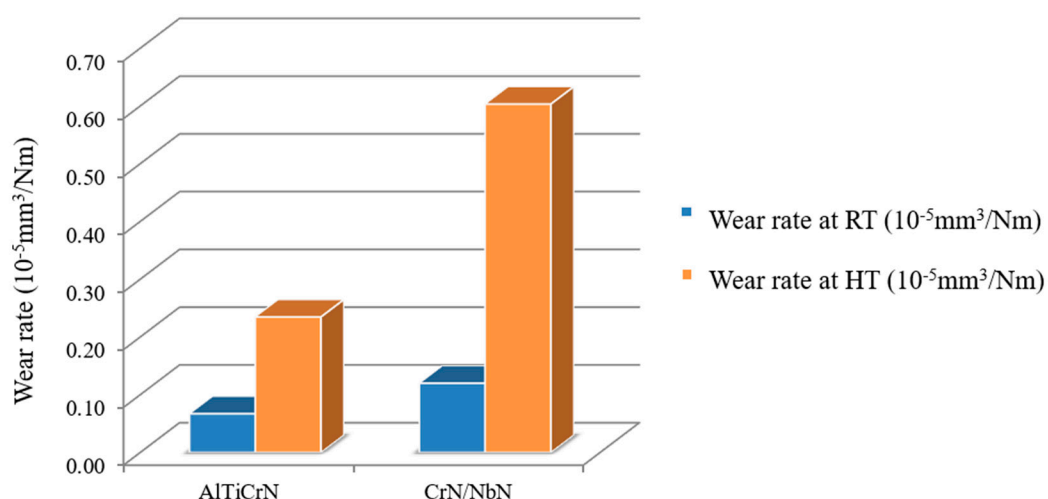


Figure 6. Values of the specific wear rate calculated after the room temperature (blue columns) and high temperature (orange columns) wear tests. Wear rates are calculated using the mean wear volume obtained from all the tested samples of each condition.

The wear rate of the superlattice CrN/NbN coating was remarkably higher than that of the AlTiCrN coatings, under both temperature regimes, with a W value after the RT tests approximately three times higher than the multilayer (AlTiCrN) one (Figure 6). However, it is important to point out that there was a significant increase in the wear rate of the multilayer coatings at HT, with the wear rate being almost twice the value obtained after the RT tribotest.

4. Discussion

The COF curves reported in Figure 2 showed that at RT the superlattice coating undergoes a significant COF reduction (Figure 2a). This can be related to the generation of a high amount of wear debris (Figure 4a,b) linked to the partial coating removal, which, under the imposed testing conditions, is likely to act as solid lubricants, while highlighting a remarkable lack of adhesion. While microscopy

(Figure 4b), profilometry (Figure 4d), and microanalysis results (Figure 5d) highlighted high plastic deformation and the complete removal of the Cr/N/NbN coating, the HT tribotest (Figure 2b) showed no remarkable variations during the sliding. A reasonable explanation of this can be ascribed to a coating removal process occurring at the very beginning of the test, consistent with the thermal stability limit reached by the present coating at the imposed temperature level. A spallation phenomenon was detected on the inner side of the AlTiCrN coating at RT in Figure 3a, but no evidence of it was observed in the EDS line scans (Figure 5a), meaning that the wear track was smooth, but the wear and the wear debris accumulation were not uniform.

Previous studies performed on the same samples by some of the authors in the present study [64,78] showed that upon thermal cycling at 873 K, the superlattice CrN/NbN coating showed oxidation and hardness decay, while the multilayer AlTiCrN coating showed high oxidation resistance with a stable high degree of hardness. The mechanical properties (hardness and elastic modulus) of the coatings were also investigated by nanoindentation in previous papers published by some of the authors in the present study [64,78]. According to these results, the resistance to plastic deformation, which is described by the ratio H^3/E^2 [79], resulted in ~ 0.146 for the CrN/NbN coating and ~ 0.153 for the AlTiCrN at RT. The lower value of the superlattice coating can be related to the degradation of the CrN/NbN coatings during the RT wear test, the related generation of wear debris which led to the peculiar trend of the COF (Figure 2a) and to the consequent abrasive wear mechanism. Despite the ability to accommodate the deformation of the HSS substrate shown by the superlattice coating upon thermal cycling, thickness reduction and oxidation phenomena appeared to play a key role during the HT wear test, where plastic deformation was suggested to be the main reason of failure. Compared to the literature [80–82], the results of the RT and HT wear performance of the particular superlattice CrN/NbN coating used in the present study highlighted that the unique extreme testing conditions applied allows us to assess its limitations in terms of thermo-mechanical challenging applications.

The chemical composition of the AlTiCrN coatings make them particularly suitable for high-temperature applications, owing to the addition of chromium [83–85]. However, despite this background information, the application of extreme working conditions, such as those used in the present paper, showed that temperature seems to have a remarkable effect on both the wear rate and the surface of the coatings, leading to high wear debris formation. The applied HT testing conditions resulted in an overall softening effect of the multilayer coating, resulting in a lower COF (Figure 2b) with respect to the RT value, but also led to a higher wear rate (Figure 6) and plastic deformation. On the other hand, the wear performance at RT, governed by abrasive wear, was remarkable.

The high plastic deformation taking place during HT wear tests, together with the reduction of the coefficient of friction, is in agreement with the results reported in the literature for AlTiCrN deposited on stainless steel [60] and cemented carbide [75]. It is worth noting that during the sliding at HT against silicon nitride counterbodies, the COF evolution during the HT tribotests showed friction regimes completely different from the smooth trend reported in the present paper. On the other hand, while no signs of failure of AlTiCrN coatings on HSS substrates were observed by Jakubčzyová et al. [76], an increased COF was observed with the increasing tribotest temperature.

The calculated specific wear rate confirmed the poor wear behavior of the superlattice CrN/NbN coating under the applied testing conditions, with the sample showing the highest W values both after RT and HT tribotests (Figure 6).

5. Conclusions

In the present study, the microstructure and the wear properties of commercially available multilayer AlTiCrN and a superlattice (nanolayered) CrN/NbN coating, PVD-deposited on a S600 HSS, were characterized. Samples were subjected to tribotests at room temperature (293 K) and a high temperature (873 K), and the effects of the temperature on the tribological behavior was evaluated by FEGSEM and EDS inspections, as well as by optical profilometry. The main conclusions can be outlined as follows:

- The multilayered AlTiCrN coating exhibited the best response under the RT tribotest; on the other hand, the coating stability and friction properties were strongly affected by the HT regime, resulting in the complete removal of the coating from the S600 HSS substrate.
- The nanolayered superlattice CrN/NbN coating showed the worst overall performance under the HT tribotest, being quickly and completely removed from the substrate. Moreover, this sample showed a partial removal of the coating in the wear tracks during the RT wear test due to the applied conditions.
- Both the multilayered and the nanolayered coatings showed remarkable material removal during the HT tribotests, as well as a spallation phenomenon on the edges of the wear tracks.
- The tribotests performed at HT showed a dramatic lack of adhesion for both samples.

The particular working conditions (i.e., high working temperature, load, and speed) allowed us to characterize the multilayered AlTiCrN and the nanolayered superlattice CrN/NbN coatings, and to define their peculiar structural and tribological behaviours and limits. Therefore, further studies on the improvement of their mechanical properties and, in particular, on their adhesion to the HSS substrate under demanding working conditions, as those typical of dry tooling applications, will be carried out in the near future.

Author Contributions: Conceptualization, A.M.S.H. and F.M.; methodology, M.C. and S.S.; validation, formal analysis, and investigation, E.S. and A.P.; writing—review and editing, E.S. and M.C.

Funding: This research was made possible by an NPRP award NPRP 5–423–2–167 from the Qatar National Research Fund (a member of The Qatar Foundation). The statements made herein are solely the responsibility of the authors.

Conflicts of Interest: The authors declare no conflict of interest.

References

1. Bay, N.; Olsson, D.D.; Andreasen, J. Lubricant test methods for sheet metal forming. *Tribol. Int.* **2008**, *41*, 844–853. [\[CrossRef\]](#)
2. Benedicto, E.; Carouc, D.; Rubio, E.M. Technical, Economic and Environmental Review of the Lubrication/Cooling Systems Used in Machining Processes. *Procedia Eng.* **2017**, *184*, 99–116. [\[CrossRef\]](#)
3. Kataoka, S.; Murakawa, M.; Aizawa, T.; Ike, H. Tribology of dry deep-drawing of various metal sheets with use of ceramics tools. *Surf. Coat. Technol.* **2004**, *177–178*, 582–590. [\[CrossRef\]](#)
4. Inspektor, A.; Salvador, P.A. Architecture of PVD coatings for metalcutting applications: A review. *Surf. Coat. Technol.* **2014**, *257*, 138–153. [\[CrossRef\]](#)
5. Zega, B. Hard decorative coatings by reactive physical vapor deposition: 12 Years of development. *Surf. Coat. Technol.* **1989**, *39–40*, 507–520. [\[CrossRef\]](#)
6. Panjan, M.; Klanjšek Gunde, M.; Panjan, P.; Čekada, M. Designing the color of AlTiN hard coating through interference effect. *Surf. Coat. Technol.* **2014**, *254*, 65–72. [\[CrossRef\]](#)
7. Podgornik, B.; Zajec, B.; Bay, N.; Vižintin, J. Application of hard coatings for blanking and piercing tools. *Wear* **2011**, *270*, 850–856. [\[CrossRef\]](#)
8. Voevodin, A.A.; O'Neill, J.P.; Zabinski, J.S. Nanocomposite tribological coatings for aerospace applications. *Surf. Coat. Technol.* **1999**, *116–119*, 36–45. [\[CrossRef\]](#)
9. Aizawa, T.; Iwamura, E.; Itoh, K. Development of nano-columnar carbon coating for dry micro-stamping. *Surf. Coat. Technol.* **2007**, *202*, 1177–1181. [\[CrossRef\]](#)
10. Schmauder, T.; Nauenburg, K.-D.; Kruse, K.; Ickes, G. Hard coatings by plasma CVD on polycarbonate for automotive and optical applications. *Thin Solid Films* **2006**, *502*, 270–274. [\[CrossRef\]](#)
11. Abadías, G.; Djemia, P.H.; Belliard, L. Alloying effects on the structure and elastic properties of hard coatings based on ternary transition metal (M = Ti, Zr or Ta) nitrides. *Surf. Coat. Technol.* **2014**, *257*, 129–137. [\[CrossRef\]](#)
12. Leyland, A.; Matthews, A. On the significance of the H/E ratio in wear control: A nanocomposite coating approach to optimised tribological behavior. *Wear* **2000**, *246*, 1–11. [\[CrossRef\]](#)

13. Ni, W.; Cheng, Y.-T.; Lukitsch, M.J.; Weiner, A.M.; Lev, L.C.; Grummon, D.S. Effects of the ratio of hardness to Young's modulus on the friction and wear behavior of bilayer coatings. *Appl. Phys. Lett.* **2004**, *85*, 4028–4030. [\[CrossRef\]](#)
14. Musil, J. Hard nanocomposite coatings: Thermal stability, oxidation resistance and toughness. *Surf. Coat. Technol.* **2012**, *207*, 50–65. [\[CrossRef\]](#)
15. Guo, J.; Wang, H.; Meng, F.; Liu, X.; Huang, F. Tuning the H/E* ratio and E* of AlN coatings by copper addition. *Surf. Coat. Technol.* **2013**, *228*, 68–75. [\[CrossRef\]](#)
16. Voevodin, A.A.; Zabinski, J.S.; Muratore, C. Recent Advances in Hard, Tough, and Low Friction Nanocomposite Coatings. *Tsinghua Sci. Technol.* **2005**, *10*, 665–679. [\[CrossRef\]](#)
17. Wang, C.; Shi, K.; Gross, C.; Pureza, J.M.; de Mesquita Lacerda, M.; Chung, Y.W. Toughness enhancement of nanostructured hard coatings: Design strategies and toughness measurement techniques. *Surf. Coat. Technol.* **2014**, *257*, 206–212. [\[CrossRef\]](#)
18. Kindlund, H.; Sangiovanni, D.G.; Martinez-de-Olcoz, L.; Lu, J.; Jensen, J.; Birch, J.; Petrov, I.; Greene, J.E.; Chirita, V.; Hultman, L. Toughness enhancement in hard ceramic thin films by alloy design. *APL Mater.* **2013**, *1*, 042104. [\[CrossRef\]](#)
19. Sargade, V.G.; Gangopadhyay, S.; Paul, S.; Chattopadhyay, A.K. Effect of coating thickness and dry performance of tin film deposited on cemented carbide inserts using CFUBMS. *Mater. Manuf. Process.* **2011**, *26*, 1028–1033. [\[CrossRef\]](#)
20. Jawaid, A.; Olajire, K.A. Cuttability investigation of coated carbides. *Mater. Manuf. Process.* **1999**, *14*, 559–580. [\[CrossRef\]](#)
21. Kulkarni, A.P.; Sargade, V.G. Characterization and performance of AlTiN, AlTiCrN, TiN/TiAlN PVD coated carbide tools while turning SS 304. *Mater. Manuf. Process.* **2015**, *30*, 748–755. [\[CrossRef\]](#)
22. Singh, K.; Limaye, P.-K.; Soni, N.L.; Grover, A.K.; Agrawal, R.G.; Suri, A.K. Wear studies of (Ti–Al)N coatings deposited by reactive magnetron sputtering. *Wear* **2005**, *258*, 1813–1824. [\[CrossRef\]](#)
23. Deng, J.X.; Liu, J.H.; Zhao, J.L.; Song, W.L. Wear mechanisms of PVD ZrN coated tools in machining. *Int. J. Refract. Met. Hard Mater.* **2008**, *26*, 164–172. [\[CrossRef\]](#)
24. Wolfe, G.; Petrosky, C.; Quinto, D.T. The role of hard coatings in carbide milling tools. *J. Vac. Sci. Technol. A Vac. Surf. Films* **1986**, *4*, 2747–2754. [\[CrossRef\]](#)
25. Su, Y.L.; Kao, W.H. Optimum multilayer TiN–TiCN coatings for wear resistance and actual application. *Wear* **1998**, *223*, 119–130. [\[CrossRef\]](#)
26. Su, Y.L.; Kao, W.H. Tribological Behavior and Wear Mechanisms of TiN/TiCN/TiN Multilayer Coatings. *J. Mater. Eng. Perform.* **1998**, *7*, 601–612. [\[CrossRef\]](#)
27. Jindal, P.C.; Santhanam, A.T.; Schleinkofer, U.; Shuster, A.F. Performance of PVD TiN, TiCN, and TiAlN coated cemented carbide tools in turning. *Int. J. Refract. Met. Hard Mater.* **1999**, *17*, 163–170. [\[CrossRef\]](#)
28. Zhang, S.; Weiguang, Z. TiN coating of tool steels: A review. *J. Mater. Process. Technol.* **1993**, *39*, 165–177. [\[CrossRef\]](#)
29. Münz, W.D. Titanium aluminum nitride films: A new alternative to TiN coatings. *J. Vac. Sci. Technol. A Vac. Surf. Films* **1986**, *4*, 2717–2725. [\[CrossRef\]](#)
30. Seidl, W.M.; Bartosik, M.; Koložsvári, S.; Bolvardi, H.; Mayrhofer, P.H. Influence of coating thickness and substrate on stresses and mechanical properties of (Ti,Al,Ta)N/(Al,Cr)N multilayers. *Surf. Coat. Technol.* **2018**, *347*, 92–98. [\[CrossRef\]](#)
31. Ikeda, T.; Sato, H. Phase formation and characterization of hard coatings in the Ti–Al–N system prepared by the cathodic arc ion plating method. *Thin Solid Films* **1991**, *195*, 99–110. [\[CrossRef\]](#)
32. Knotek, O.; Münz, W.D.; Leyendecker, T. Industrial deposition of binary, ternary, and quaternary nitrides of titanium, zirconium, and aluminum. *J. Vac. Sci. Technol. A Vac. Surf. Films* **1987**, *5*, 2173–2179. [\[CrossRef\]](#)
33. Kalss, W.; Reiter, A.; Derflinger, V.; Gey, C.; Endrino, J.L. Modern coatings in high performance cutting applications. *Int. J. Refract. Met. Hard Mater.* **2006**, *24*, 399–404. [\[CrossRef\]](#)
34. Yamamoto, K.; Sato, T.; Takahara, K.; Hanaguri, K. Properties of (Ti,Cr,Al)N coatings with high Al content deposited by new plasma enhanced arc-cathode. *Surf. Coat. Technol.* **2003**, *174*, 620–626. [\[CrossRef\]](#)
35. Deng, J.; Wu, F.; Lian, Y.; Xing, Y.; Li, S. Erosion wear of CrN, TiN, CrAlN, and TiAlN PVD nitride coatings. *Int. J. Refract. Met. Hard Mater.* **2012**, *35*, 10–16. [\[CrossRef\]](#)
36. Panjan, P.; Navinsek, B.; Cekada, M.; Zalar, A. Oxidation behaviour of TiAlN coatings sputtered at low temperature. *Vacuum* **1999**, *53*, 127–133. [\[CrossRef\]](#)

37. Kawate, M.; Hashimoto, A.K.; Suzuki, T. Oxidation resistance of $\text{Cr}_{1-x}\text{Al}_x\text{N}$ and $\text{Ti}_{1-x}\text{Al}_x\text{N}$ films. *Surf. Coat. Technol.* **2003**, *165*, 163–167. [\[CrossRef\]](#)
38. Hörling, A.; Hultman, L.; Odén, M.; Sjöln, J.; Karlsson, L. Mechanical properties and machining performance of $\text{Ti}_{1-x}\text{Al}_x\text{N}$ -coated cutting tools. *Surf. Coat. Technol.* **2005**, *191*, 384–392. [\[CrossRef\]](#)
39. Kulkarni, A.P.; Joshi, G.; Sargade, V.G. Performance of PVD AlTiCrN coating during machining of austenitic stainless steel. *Surf. Eng.* **2013**, *29*, 402–405. [\[CrossRef\]](#)
40. Mayrhofer, P.H.; Hörling, A.; Karlsson, L.; Sjöln, J.; Larsson, T.; Mitterer, C.; Hultman, L. Self-organized nanostructures in the Ti–Al–N system. *Appl. Phys. Lett.* **2003**, *83*, 2049–2051. [\[CrossRef\]](#)
41. Mayrhofer, P.H.; Mitterer, C.; Hultman, L.; Clemens, H. Microstructural design of hard coatings. *Prog. Mater. Sci.* **2006**, *51*, 1032–1114. [\[CrossRef\]](#)
42. Koehler, J. Attempt to Design a Strong Solid. *Phys. Rev. B* **1970**, *2*, 547–551. [\[CrossRef\]](#)
43. Helmersson, U.; Todorova, S.; Barnett, S.A.; Sundgren, J.-E.; Markert, L.C.; Greene, J.E. Growth of single-crystal TiN/VN strained-layer superlattices with extremely high mechanical hardness. *J. Appl. Phys.* **1987**, *62*, 481–484. [\[CrossRef\]](#)
44. Münz, W.D. Large-scale manufacturing of nanoscale multilayered hard coatings deposited by cathodic arc/unbalanced magnetron sputtering. *MRS Bull.* **2003**, *28*, 173–179. [\[CrossRef\]](#)
45. Hovsepian, P.E.; Lewis, D.B.; Münz, W.D. Recent progress in large scale manufacturing of multilayer/superlattice hard coatings. *Surf. Coat. Technol.* **2000**, *133–134*, 166–175. [\[CrossRef\]](#)
46. Hovsepian, P.E.; Münz, W.D. Recent progress in large-scale production of nanoscale multilayer/superlattice hard coatings. *Vacuum* **2003**, *69*, 27–36. [\[CrossRef\]](#)
47. Lewis, D.B.; Hovsepian, P.E.; Schönjahn, C.; Ehasarian, A.; Smith, I.J. Industrial scale manufactured superlattice hard PVD coatings. *Surf. Eng.* **2001**, *17*, 15–27.
48. Luo, Q.; Lewis, D.B.; Hovsepian, P.E.; Münz, W.D. Transmission Electron Microscopy and X-ray Diffraction Investigation of the Microstructure of Nanoscale Multilayer TiAlN/VN Grown by Unbalanced Magnetron Deposition. *J. Mater. Res.* **2004**, *19*, 1093–1104. [\[CrossRef\]](#)
49. Luo, Q.; Hovsepian, P.E.; Lewis, D.B.; Münz, W.D.; Kok, Y.N.; Cockrem, J.; Bolton, M.; Farinotti, A. Tribological properties of unbalanced magnetron sputtered nano-scale multilayer coatings TiAlN/VN and TiAlCrYN deposited on plasma nitrided steels. *Surf. Coat. Technol.* **2005**, *193*, 39–45. [\[CrossRef\]](#)
50. Luo, Q.; Zhou, Z.; Rainforth, W.M.; Hovsepian, P.E. TEM-EELS study of low-friction superlattice TiAlN/VN coating: The wear mechanisms. *Tribol. Lett.* **2006**, *24*, 171–178. [\[CrossRef\]](#)
51. Barshilia, H.C.; Deepthi, B.; Rajam, K.S. Growth and characterization of TiAlN/CrAlN superlattices prepared by reactive direct current magnetron sputtering. *J. Vac. Sci. Technol. A Vac. Surf. Films* **2009**, *27*, 29–36. [\[CrossRef\]](#)
52. Barshilia, H.C.; Rajam, K.S.; Jain, A.; Gopinadhan, K.; Chaudhary, S. A comparative study on the structure and properties of nanolayered TiN/NbN and TiAlN/TiN multilayer coatings prepared by reactive direct current magnetron sputtering. *Thin Solid Films* **2006**, *503*, 158–166. [\[CrossRef\]](#)
53. Yana, S.; Fua, T.; Wang, R.; Tian, C.; Wang, Z.; Huang, Z.; Yang, B.; Fu, D. Deposition of CrSiN/AlTiSiN nano-multilayer coatings by multi-arc ion plating using gas source silicon. *Nucl. Instrum. Methods Phys. Res. Sect. B* **2013**, *307*, 143–146. [\[CrossRef\]](#)
54. Münz, W.D.; Donohue, L.A.; Hovsepian, P.E. Properties of various large-scale fabricated TiAlN- and CrN-based superlattice coatings grown by combined cathodic arc–unbalanced magnetron sputter deposition. *Surf. Coat. Technol.* **2000**, *125*, 269–277. [\[CrossRef\]](#)
55. Patel, N.; Wang, S.; Inspektor, A.; Salvador, P.A. Secondary hardness enhancement in large period TiN/TaN superlattices. *Surf. Coat. Technol.* **2014**, *254*, 21–27. [\[CrossRef\]](#)
56. An, J.; Zhang, Q.Y. Structure, hardness and tribological properties of nanolayered TiN/TaN multilayer coatings. *Mater. Charact.* **2007**, *58*, 439–446. [\[CrossRef\]](#)
57. Shugurov, A.R.; Kazachenok, M.S. Mechanical properties and tribological behavior of magnetron sputtered TiAlN/TiAl multilayer coatings. *Surf. Coat. Technol.* **2018**, *353*, 254–262. [\[CrossRef\]](#)
58. Ramadoss, R.; Kumar, N.; Dash, S.; Arivuoli, D.; Tyagi, A.K. Wear mechanism of CrN/NbN superlattice coating sliding against various counterbodies. *Int. J. Refract. Met. Hard Mater.* **2013**, *41*, 547–552. [\[CrossRef\]](#)
59. Santecchia, E.; Hamouda, A.M.S.; Musharavati, F.; Zalnezhad, E.; Cabibbo, M.; Spigarelli, S. Wear resistance investigation of titanium nitride-based coatings. *Ceram. Int.* **2015**, *41*, 10349–10379. [\[CrossRef\]](#)

60. Zhou, H.; Zheng, J.; Gui, B.; Geng, D.; Wang, Q. AlTiCrN coatings deposited by hybrid HIPIMS/DC magnetron co-sputtering. *Vacuum* **2017**, *136*, 129–136. [CrossRef]
61. Holmberg, K.; Matthews, A. *Coatings Tribology*, 2nd ed.; Elsevier: Amsterdam, The Netherlands, 2009.
62. Haubner, R.; Lessiak, M.; Pitonak, R.; Köpf, A.; Weissenbacher, R. Evolution of conventional hard coatings for its use on cutting tools. *Int. J. Refract. Met. Hard Mater.* **2017**, *62*, 210–218. [CrossRef]
63. Bobzin, K. High-performance coatings for cutting tools. *CIRP J. Manuf. Sci. Technol.* **2017**, *18*, 1–9. [CrossRef]
64. Cabibbo, M.; El Mehtedi, M.; Clemente, N.; Spigarelli, S.; Hamouda, A.M.S.; Musharavati, F.; Daurù, M. High temperature thermal stability of innovative nanostructured thin coatings for advanced tooling. *Key Eng. Mater.* **2014**, 622–623, 45–52. [CrossRef]
65. Lafer Company Website. Available online: <http://www.lafer.eu/en/technical-notes/> (accessed on 30 January 2019).
66. Bhushan, B. *Modern Tribology Handbook*, 1st ed.; CRC Press: Boca Raton, FL, USA, 2000.
67. Aihua, L.; Jianxin, D.; Haibing, C.; Yangyang, C.; Jun, Z. Friction and wear properties of TiN, TiAlN, AlTiN and CrAlN PVD nitride coatings. *Int. J. Refract. Met. Hard Mater.* **2012**, *31*, 82–88. [CrossRef]
68. Yang, S.; Wiemann, E.; Teer, D.G. The properties and performance of Cr-based multilayer nitride hard coatings using unbalanced magnetron sputtering and elemental metal targets. *Surf. Coat. Technol.* **2004**, 188–189, 662–668. [CrossRef]
69. Yang, S.; Teer, D.G. Properties and performance CrTiAlN of multilayer hard coatings deposited using magnetron sputter ion plating. *Surf. Eng.* **2002**, *18*, 391–396. [CrossRef]
70. Eh Hovsepian, P.; Ehasarian, A.P.; Purandare, Y.P.; Mayr, P.; Abstoss, K.G.; Mosquera Feijoo, M.; Schulz, W.; Kranzmann, A.; Lasanta, M.I.; Trujillo, J.P. Novel HIPIMS deposited nanostructured CrN/NbN coatings for environmental protection of steam turbine components. *J. Alloy. Compd.* **2018**, *746*, 583–593. [CrossRef]
71. Hovsepian, P.E.; Ehasarian, A.P.; Purandare, Y.P.; Biswas, B.; Pérez, F.J.; Lasanta, M.I.; de Miguel, M.T.; Illana, A.; Juez-Lorenzo, M.; Muelas, R.; et al. Performance of HIPIMS deposited CrN/NbN nanostructured coatings exposed to 650 °C in pure steam environment. *Mater. Chem. Phys.* **2016**, *179*, 110–119. [CrossRef]
72. Agüero, A.; Juez-Lorenzo, M.; Hovsepian, P.E.; Ehasarian, A.P.; Purandare, Y.P.; Muelas, R. Long-term behaviour of Nb and Cr nitrides nanostructured coatings under steam at 650 °C. Mechanistic considerations. *J. Alloy. Compd.* **2018**, *739*, 549–558. [CrossRef]
73. Strahin, B.L.; Doll, G.L. Tribological coatings for improving cutting tool performance. *Surf. Coat. Technol.* **2018**, *336*, 117–122. [CrossRef]
74. Kalin, M.; Jerina, J. The effect of temperature and sliding distance on coated (CrN, TiAlN) and uncoated nitrided hot-work tool steels against an aluminium alloy. *Wear* **2015**, *330–331*, 371–379. [CrossRef]
75. Dejun, K.; Guizhong, F. Friction and wear behaviors of AlTiCrN coatings by cathodic arc ion plating at high temperatures. *J. Mater. Res.* **2015**, *30*, 503–511. [CrossRef]
76. Jakubéczyová, D.; Hvizdos, P.; Selecká, M. Investigation of thin layers deposited by two PVD techniques on high speed steel produced by powder metallurgy. *Appl. Surf. Sci.* **2012**, *258*, 5105–5110. [CrossRef]
77. Ma, D.; Ma, S.; Dong, H.; Xu, K.; Bell, T. Microstructure and tribological behaviour of super-hard Ti–Si–C–N nanocomposite coatings deposited by plasma enhanced chemical vapour deposition. *Thin Solid Films* **2006**, *496*, 438–444. [CrossRef]
78. Cabibbo, M.; Clemente, N.; El Mehtedi, M.; Spigarelli, S.; Daurù, M.; Hammuda, A.S.; Musharavati, F. Mechanical and microstructure characterization of hard nanostructured N-bearing thin coating. *Metall. Ital.* **2015**, *5*, 5–9.
79. Tsui, T.Y.; Pharr, G.M.; Oliver, W.C.; Bhatia, C.S.; White, R.L.; Anders, S.; Anders, A.; Brown, I.G. Nanoindentation and nanoscratching of hard carbon coatings for magnetic discs. *MRS Online Proc.* **1995**, *383*, 447–452. [CrossRef]
80. Huang, W.; Zalnezhad, E.; Musharavati, F.; Jahanshahi, P. Investigation of the tribological and biomechanical properties of CrAlTiN and CrN/NbN coatings on SST 304. *Ceram. Int.* **2017**, *43*, 7992–8003. [CrossRef]
81. Bemporad, E.; Pecchio, C.; De Rossi, S.; Carassiti, F. Characterisation and wear properties of industrially produced nanoscaled CrN/NbN multilayer coating. *Surf. Coat. Technol.* **2004**, 188–189, 319–330. [CrossRef]
82. Savisalo, T.; Lewis, D.B.; Luo, Q.; Bolton, M.; Hovsepian, P.E. Structure of duplex CrN/NbN coatings and their performance against corrosion and wear. *Surf. Coat. Technol.* **2008**, *202*, 1661–1667. [CrossRef]
83. Bai, L.; Zhu, X.; Xiao, J.; He, J. Study on thermal stability of CrTiAlN coating for dry drilling. *Surf. Coat. Technol.* **2007**, *201*, 5257–5260. [CrossRef]

84. Zhou, Z.F.; Tam, P.L.; Shum, P.W.; Li, K.Y. High temperature oxidation of CrTiAlN hard coatings prepared by unbalanced magnetron sputtering. *Thin Solid Films* **2009**, *517*, 5243–5247. [[CrossRef](#)]
85. Tam, P.L.; Zhou, Z.F.; Shum, P.W.; Li, K.Y. Structural, mechanical, and tribological studies of Cr–Ti–Al–N coating with different chemical compositions. *Thin Solid Films* **2008**, *516*, 5725–5731. [[CrossRef](#)]



© 2019 by the authors. Licensee MDPI, Basel, Switzerland. This article is an open access article distributed under the terms and conditions of the Creative Commons Attribution (CC BY) license (<http://creativecommons.org/licenses/by/4.0/>).